

Composition control of tin–zinc deposits using experimental strategies

Chi-Chang Hu ^{*,1}, Chun-Kou Wang, Gen-Lan Lee

Department of Chemical Engineering, National Chung Cheng University, Chia-Yi 621, Taiwan

Received 21 July 2005; received in revised form 17 October 2005; accepted 18 October 2005

Available online 28 November 2005

Abstract

The robust electroplating settings of a direct-current (dc) plating mode for the co-deposition of Sn–Zn deposits with their composition close to the eutectic point (i.e., Sn–9Zn) from the chloride solutions were achieved and investigated by using experimental strategies, including the fractional factorial design (FFD) and central composite design (CCD) coupled with the response surface methodology (RSM). The temperature of the plating bath, pH, and the metallic ion ratio (i.e., Sn⁴⁺/Zn²⁺ ratio) were found to be the key factors affecting the composition of Sn–Zn deposits in the FFD study. The effects of pH and temperature of the plating solution on the composition of Sn–Zn deposits were examined using a regression model in the CCD study. This model, represented as contour plots, showed that pH 5.0 and temperature = 78 °C were the robust electroplating settings for the co-deposition of the eutectic Sn–Zn alloys, which was independent of the substrates. In addition, based on the robust plating settings, the composition of Sn–Zn alloys could be precisely controlled and predicted by adjusting the composition of the plating baths. From the morphologies and crystalline information, the binary Sn–Zn deposits prepared in this work should belong to heterogeneous alloys.
© 2005 Elsevier Ltd. All rights reserved.

Keywords: Electroplating; Sn–Zn deposit; Eutectic point; Fractional factorial design; Central composite design

1. Introduction

The flip–chip bonding is one of various surface-mounting techniques in the integrated circuit (IC) assembly industry, which was developed to provide high-density interconnections between the chip and the substrate [1]. The flip–chip bonding process entails (1) disposing a plurality of solder bumps on the upper-surface of the die that is mounted directly to the substrate, (2) flipping the die and mating the solder bumps with the corresponding bonding Al pads located on the substrate, and (3) heating the die and the substrate in order to reflow the solder bumps. Each reflowed bump forms a bond between the die and the substrate, which functions as an electrical and physical contact.

In general, tin–lead (Sn–Pb) solder was widely used as the bump material for the flip–chip packaging applications [2–4], which was originally deposited by means of a vacuum evaporation technique developed by IBM [1]. However, a variety of new methods/processes were developed to form solder bumps,

especially the electroplating process [4–6], in order to increase the density of interconnections. Recently, lead-free processes for electronic devices and components are required to address the environmental concerns and the alpha radiation of impurities of Pb [7–9]. In addition, the demand of Pb-free bumps rather than Sn–Pb solder becomes an urgent problem in the electronic assembly industry. Therefore, different types of Pb-free solder bump materials have been investigated, which are generally the tin-rich, eutectic alloys (e.g., Sn–Ag, Sn–Cu, Sn–Ag–Cu, Sn–Bi, Sn–Zn, etc.) [7–10]. Among these eutectic Sn-rich alloys, Sn–9Zn generally shows the advantages of a low reflowing temperature (an eutectic point of 198 °C), low cost, high wetting capability, good malleability, and a high anti-corrosive property. Accordingly, this work focuses on the electroplating and composition control of the Sn–Zn deposits with their composition close to the eutectic point.

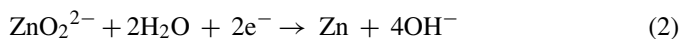
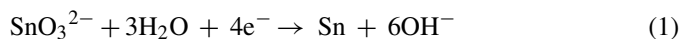
Electroplating is recognized to be suitable for making the fine pitch bumps with high-speed deposition and high reliability [7,8,11,12]. In addition, this deposition technique attracts industrial considerations because of the low cost, the high throughput, and the deposition capability on almost any geometry [13]. Moreover, electroplating is a simple, one-step process for the fabrication of Sn–Pb solders for printed circuit boards, solder bumps, and lead-frame packages in the electronic applications.

* Corresponding author. Tel.: +886 5 2720411x33411; fax: +886 5 2721206.
E-mail address: chmhcc@ccu.edu.tw (C.-C. Hu).

¹ ISE member.

Accordingly, it is worthy being paid attention on the production of lead-free bump interconnections by means of the electroplating technologies [7,8,10–12].

According to Brenner's definition [14], the co-deposition of Sn–Zn alloys from the cyanide-based baths belongs to the alloy electroplating of the irregular type since the effects of the plating temperature and current density on the composition of Sn–Zn are irregular. In this work, however, cyanide is not employed and thus, the reaction mechanism is generally proposed as following:



Based on the fact that Sn(II) is easily oxidized to Sn(IV) under air agitation in high-temperature plating solutions, a chloride-based Sn(IV) bath is employed in this work.

The experimental strategy is a sequential procedure to reach the optimal operation conditions of interest [15–20]. Based on this strategy, the response variable(s) (e.g., the Sn content in the Sn–Zn alloys) is a function of the quantitative control variables. Since the starting point of experimental conditions is usually remote from the optimum meanwhile there may be several key factors influencing the response(s) of interest, the fractional factorial design (FFD) is usually employed to efficiently find these key variables [15–17]. From the FFD, the response variable(s) against the key factors near the starting point in the system is simply fitted as a first-order model. After the FFD experiment, the methodology of the steepest ascent path is often used to approach the vicinity of the optimal conditions if the starting point of experimental conditions is really far from the optimum. Finally, the central composite design (CCD) is used to model the apparent curvature of response variable(s) against the key factors at the vicinity of optimum. Since mathematic models of the response variable(s) against the control variables can be represented as contour lines or a plane in graphs, this method is called a response surface methodology (RSM).

The purpose of this work is to identify the suitable electroplating conditions to produce Sn–Zn deposits with the composition close to the eutectic point (i.e., Sn–9Zn). The key variables affecting the composition of Sn (and Zn) in the Sn–Zn deposits were screened out by the FFD [15–17]. These variables were subjected to the CCD coupled with the RSM [15,16] to examine the relationship between the composition of Sn–Zn alloys and the plating variables around the optimal plating conditions of Sn–9Zn deposits. Finally, the proposed plating settings were applied to deposit Sn–9Zn alloys onto various substrates (i.e., Fe, Ni, and Cu) to demonstrate the robust property.

2. Experimental details

Tin–zinc deposits were electroplated onto commercially pure (99.5%) 1 cm × 2 cm copper plates or the Cu plates deposited with a thin film of either Fe or Ni. The copper plates were first cleaned with trichloroethylene, rinsed with pure water, and then, anodized at 30 mA/cm² in a 0.1 M NaOH solution for 5 min. After anodizing, the plates were cathodically polarized at 75 mA/cm² in another 0.1 M NaOH solution for 10 s, vibrated in

Table 1

Composition and variables for the electroplating of a nickel film from a watts nickel bath

Compounds/variables	Concentration/conditions
NiSO ₄ ·6H ₂ O (mol/dm ³)	1
NiCl ₂ ·6H ₂ O (mol/dm ³)	0.2
H ₃ BO ₃ (mol/dm ³)	0.5
Temperature (°C)	55
pH ^a	3.8
Current density (mA/cm ²)	60

^a pH was adjusted by 1 M HCl or NaOH.

an ultrasonic bath for 5 min, acid-cleaned with 5 M H₂SO₄ for 1 min. Finally, the Cu substrates were rinsed with pure water and vibrated in an ultrasonic bath for 5 min. For the substrates with Ni or Fe thin films (denoted as Ni/Cu and Fe/Cu, respectively), the pre-cleaned Cu substrate was vertically placed in a 500-ml jacket cell with a watts nickel bath (see Table 1) or a solution containing 0.5 M FeSO₄·7H₂O + 0.1 M H₃BO₄ with pH 2.0. The Cu substrate was surrounded with an anode of platinum-coated stainless steel mesh. After the electroplating of Ni or Fe at 60 mA/cm² for 5 min under 55 °C, the substrates were rinsed with pure water. These substrates were vertically placed in another 500-ml jacket cell surrounded with an anode of platinum-coated stainless steel mesh and electroplated with Sn–Zn deposits at 80 mA/cm² for 20 min. After the Sn–Zn deposition, these electrodes were rinsed with pure water and vibrated in an ultrasonic bath for 5 min.

The plating bath mainly consisted of SnCl₄·nH₂O, ZnCl₂, and Ca(C₆H₁₁O₇)₂·H₂O (0.1 M, complex agent) with pH being adjusted with 1 M HCl and 1 M NaOH. All solutions were prepared with pure water produced by a reagent water system (Milli-Q SP, Japan) at 18 MΩ cm and all reagents were Merck, GR. Solution temperature was maintained at the specified temperatures with an accuracy of 0.1 °C by means of a water thermostat (Haake DC3 and K20).

The average composition of all deposits was measured using an energy-dispersive X-ray (EDX) spectroscope with standards at five points coupled with a scanning electron microscope (SEM, JEOL JSM35). The mean error of this EDX analysis is ca. ±1.5 atomic percents (at%).

3. Results and discussion

3.1. Fractional factorial design

To efficiently find the key variables affecting the Sn (and Zn) content in the Sn–Zn deposits, the fractional factorial design is introduced to screen out these key variables. This experiment design can observe the influences of each preparation variable at a variety of other variable levels as well as the interactions among these variables on the composition of Sn (and Zn). Based on the literature review, the effects of the following electroplating variables were investigated in the FFD study: (A) pH of the plating solution, (B) total concentration of metal ions (M), (C) temperature of the plating solution (°C), (D) [Sn⁴⁺]/[Zn²⁺] molar ratio, and (E) agitation rate (rpm). Note that in our preliminary study, the effect of the current density on the composition of Sn–Zn

Table 2
Factors and levels for 2^{5-1} fractional factorial design

Factor	Level	
	–	+
A. pH	6.0	7.0
B. Total concentration (M)	0.1	0.2
C. Temperature ($^{\circ}\text{C}$)	20	70
D. $[\text{Sn}^{4+}]/[\text{Zn}^{2+}]$ (atomic ratio)	80/20	90/10
E. Agitation rate (rpm)	10	20

deposits is insignificant. In addition, the effect of the current density on the composition of Sn–Zn deposits was found to be obviously minor, even in the cyanide-based baths [14]. Accordingly, the current density of electroplating is set at 80 mA/cm² to achieve high-speed deposition. The fixed levels of these five variables are listed in Table 2 meanwhile the 2^{5-1} design matrix with the experimental data were given in Table 3.

A 2^{k-1} fractional factorial design matrix can be constructed by writing down a basic design matrix consisting of a full 2^{k-1} factorial design and then adding the k th factor by identifying its plus and minus levels with the plus and minus signs of the highest order interaction ABC...($k-1$). For example, the 2^{5-1} fractional factorial design with the defining relation, $I = ABCDE$ (introduced by Box et al. [17]), shows the following property:

$$E = E \cdot I = E \cdot ABCDE = ABCDE^2 = ABCD \quad (3)$$

Therefore, the 2^{5-1} fractional factorial design is obtained by writing down the full 2^4 factorial as the basic design and then equating factor E to the ABCD interaction [16]. According to Eq. (3), the orthogonal contrast coefficients of factor E are equal to that of the ABCD interaction. In addition, the combination of observations used to estimate the effect of factor E (agitation rate) is identical to that used to estimate the four-factor interaction effect of the aliases A (pH of the plating solution), B (total concentration of metal ions), C (temperature of the plating solu-

Table 3
The design matrix and experimental data of the average Sn content in the Sn–Zn deposits for 2^{5-1} fractional factorial design with the defining relation $I = ABCDE$

Run	Factors					Sn content (wt%)
	A	B	C	D	E	
1	–	–	–	–	+	23.4
2	+	–	–	–	–	17.2
3	–	+	–	–	–	16.5
4	+	+	–	–	+	28.2
5	–	–	+	–	–	68.8
6	+	–	+	–	+	70.1
7	–	+	+	–	+	71.4
8	+	+	+	–	–	73.3
9	–	–	–	+	–	30.3
10	+	–	–	+	+	53.4
11	–	+	–	+	+	43.9
12	+	+	–	+	–	49.0
13	–	–	+	+	+	85.7
14	+	–	+	+	–	92.8
15	–	+	+	+	–	84.3
16	+	+	+	+	+	92.9

Table 4
Analysis of variance for the average Sn content in the Sn–Zn deposits from the 2^{5-1} fractional factorial design

Source	SS	d.f.	MS	F^*
A	175.6	1	175.6	19.7
C	8920.8	1	8920.8	1001.5
D	1660.6	1	1660.6	186.4
E	82.8	1	82.8	9.3
AD	75.7	1	75.7	8.5
CE	78.3	1	78.3	8.8
Error	80.2	9	8.9	
Total	11073.9	15		

Remark: $F_{0.01}(1, 9) = 10.56$; $F_{0.05}(1, 9) = 5.12$; $R^2 = 1 - (\text{SSE}/\text{SST}) = 0.993$.

tion), and D ($[\text{Sn}^{4+}]/[\text{Zn}^{2+}]$ ratio). Thus, the effects of factor E and ABCD interaction are said to be confounded [15,16]. From the principle of the sparsity of effects [16], a system is likely to be driven primarily by the effects of certain main factors and low-order interactions. Thus, effects of the high-order (e.g., three and higher order) interactions are assumed to be negligible and hence, the effect of factor E can be isolated from the confounded effects by this FFD experiment (resolution = V) [16].

In Table 3, the low and high levels of A, B, C, D, and E were denoted as “–” and “+”, respectively. The contrast coefficients of factor E (i.e., column 6 in Table 3) is generated from the contrast coefficients of factors A, B, C, and D through Eq. (3). From an examination of the results in Table 3, the composition of Sn–Zn deposits is ranged from 16.5 to 92.9 at%, indicating that certain factors and/or interactions should show significant effect on the Sn content in the Sn–Zn deposits. Accordingly, analysis of variance (ANOVA) was carried out on the basis of the data shown in Table 3 and the result of the statistical analysis is summarized in Table 4. The analysis of variance (ANOVA) is derived from partitioning the total variability (SST) into its component parts (i.e., sums of square for model and error, SS_{model} and SSE, respectively), which can be calculated on the basis of the following equations [16]:

$$\text{SST} = \sum_{i=1}^{2^{k-1}} (y_i - \bar{y})^2 \quad (4)$$

$$\text{SS}_i = \frac{(C_i)^2}{2^{k-1}} \quad (5)$$

$$\text{SSE} = \text{SST} - \text{SS}_{\text{model}} \quad (6)$$

where y_i and \bar{y} are indicative of the i th response and the grand average of all the observations, respectively. Note that C_i is indicative of the contrast of factor (or interaction) i , which is the sum of multiplying the observations (i.e., y_i) with the appropriate contrast coefficients (i.e., the plus–minus signs in the appropriate column of the design matrix). In addition, SS_i indicates the sum of square corresponding to factor (or interaction) i . The sum of SS_i with the statistical significance is defined as the SS_{model} . The quantities $\text{MS}_i = \frac{\text{SS}_i}{\text{d.f.}_i}$ and $\text{MSE} = \frac{\text{SSE}}{\text{d.f.}_{\text{error}}}$ are defined as the mean squares of factor (or interaction) i and the mean square of error, respectively. The d.f._i and $\text{d.f.}_{\text{error}}$ indicate the degree of

freedom for factor (or interaction) i and error, respectively. In Table 4, the test statistics, F^* , defined as MS_i/MSE , are employed to test the statistical significance of each factor and the two-factor interactions. If the calculated value of F^* is greater than that in the F table at a specific probability level (e.g., $\alpha = 0.01$), a statistically significant factor or interaction is obtained. After the test, only factors A, C, and D exhibit statistically significant effects on the composition of Sn–Zn deposits. Actually, factor E as well as interactions AD and CE are considered as the factor/interactions with marginal significance (i.e., their effects are not as important as the effects of factors A, C, and D) since their calculated F values are somewhat lower than the critical value ($F_{0.01}(1, 9) = 10.56$). The multiple correlation coefficient, $R^2 = 1 - (SSE/SST)$, is the proportion of sum of squares of total variances (SST) explained by the fitted equation. A R^2 value close to 1 means a good fit to the experiment data. In this work, $R^2 = 0.993$, an excellent fitting, when factors A, C, D, and E as well as interactions AD and CE are considered to be significant and the other effects (including factor B and other two-factor interactions) can be pulled into the error.

Calculation of the estimates for factors and two-factor interactions is followed the procedure recommended by Box et al. [17], which is equal to $C_i/2^{k-2}$. The estimates of all factors A–E and interactions with marginal significance are shown in Fig. 1. From Table 4 and Fig. 1, it is very clear that the sequence of factors/interactions with respect to decreasing the influence is: $C > D > A > E > CE > AD$ although the last three factors show the marginal statistical significance from Table 4. Based on the results of Table 4 and Fig. 1a, an increase in pH will enhance the tin content in the Sn–Zn deposits. This effect, however, is conflict to the results obtained from the cyanide-based solutions [14,21,22], presumably due to the complicated interactions among metal ions, OH^- , and cyanide. Since factor B shows no significant effect, the variation in the total concentration of metal ions has no influence on the composition of Sn–Zn deposits. This result may be indicative of that the co-deposition of Sn–Zn alloys from the non-cyanide baths used in this work belongs to the alloy co-deposition of a regular type [14]. This proposal is also supported by the insignificant effect of the current density of electroplating on the composition of Sn–Zn deposits since the regular co-deposition process is defined as the electroplating under the control of diffusion phenomena [14]. Factor C shows the largest effect, indicating that the increase in the plating temperature from 20 to 70 °C largely promotes the Sn content from ca. 33 to 80 at%. In general, effects of the electroplating temperature on the Sn–Zn deposition include an increase in the current efficiencies of both Sn and Zn and an increase in the Sn content [22,23]. Furthermore, an additional merit of the non-cyanide baths is the absence of a rapid decomposition of cyanide at temperatures ≥ 65 °C [14]. The $[\text{Sn}^{4+}]/[\text{Zn}^{2+}]$ ratio, i.e., factor D, shows a positive effect on the composition of the Sn deposits. This also supports that the co-deposition of Sn–Zn alloys from the non-cyanide baths belongs to the alloy co-deposition of a regular type. Since factor E shows a marginal effect, varying the agitation rate should change the thickness of the diffusion layer, which renders a minor variation in the relative current efficiency for the deposition of Sn and Zn.

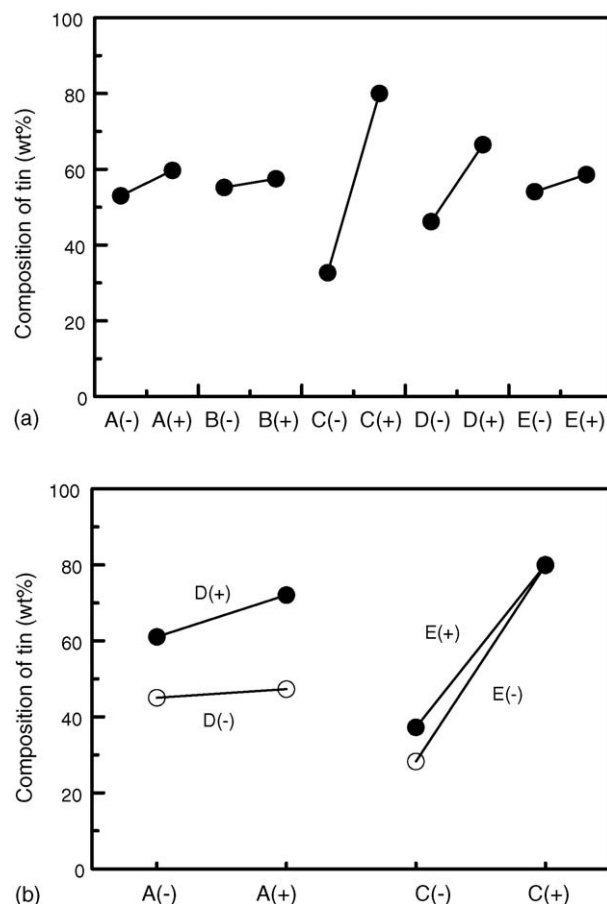


Fig. 1. Effects of (a) factors (A) pH, (B) total concentration of metal ions (M), (C) temperature of the plating bath (°C), (D) $[\text{Sn}^{4+}]/[\text{Zn}^{2+}]$ ratio, and (E) agitation rate (rpm) and (b) interactions AD and CE on the average Sn content of Sn–Zn deposits, where (+) and (–) indicate the high and low levels of factors, respectively.

The interaction effects with marginal significance (i.e., AD and CE) are shown in Fig. 1b. In this figure, for the plating solution with a high $[\text{Sn}^{4+}]/[\text{Zn}^{2+}]$ ratio (i.e., 90/10), increasing pH of the plating solution leads an obvious increase in the Sn content in the Sn–Zn deposits. However, when factor D is under the low level, pH has no effect on the Sn content. The above phenomena reveal the existence of an interaction between factors A and D. Another CE interaction effect indicates that the effect of C is more obvious when factor E is under the low level in comparison with that as factor E is under the high level. From all the above results and discussion, the composition of Sn–Zn deposits is not only dominated by the plating temperature but also by pH and the $[\text{Sn}^{4+}]/[\text{Zn}^{2+}]$ ratio in the plating solution.

From the analysis of variance and regression analysis of the results shown in Table 3, a fitted polynomial model (including the marginal effects) can be generated. This model, quantitatively elucidating the effects of all plating variables with statistical significance, is expressed in the following:

$$y = 56.4 + 3.3x_A + 23.7x_C + 10.2x_D + 2.3x_E + 2.2x_Ax_D - 2.2x_Cx_E \quad (7)$$

where x_i are the coded variables for factor i (i.e., A, C, and D). The coded variables, x_i , are defined in the standardized form as following [15]:

$$x_{i,HIGH} = \frac{(X_{i,HIGH} - X_{i,MEAN})}{S_i} (= +1) \quad (8)$$

$$x_{i,LOW} = \frac{(X_{i,LOW} - X_{i,MEAN})}{S_i} (= -1) \quad (9)$$

$$X_{i,MEAN} = \frac{(X_{i,HIGH} + X_{i,LOW})}{2} \quad (10)$$

$$S_i = \frac{(X_{i,HIGH} - X_{i,LOW})}{2} \quad (11)$$

where $X_{i,HIGH}$ and $X_{i,LOW}$ are the high and low levels of factor i in the natural unit, respectively. Note that when x_A , x_C , and x_D are equal to +1 (i.e., factors A, C, and D are in the high level), the predicted value of y (i.e., the Sn content) is equal to 93.6 that is higher than the eutectic point of Sn–Zn alloys (i.e., 91 at% Sn). Accordingly, there is no need to carry out the steepest ascent study from the results and discussion of the FFD study. Moreover, from an examination of Table 3, the experimental settings of runs 13/15 or runs 14/16 should be very close to the optimal conditions for the electroplating of eutectic Sn–9Zn deposit. Accordingly, the experimental settings of run 15 are considered as the center point in the central composite design study coupled with the response surface method [15,16]. It is worthy noting that the Sn contents of runs 13–16 shown in Table 3 are above 84 at% that is very close to the composition of metal ions in the plating baths. Therefore, the response variable (i.e., the Sn content in the Sn–Zn deposits) is considered to be a smooth function of the plating variables, which is consistent with the prediction of Eq. (7).

3.2. Central composite design

The purpose of the central composite design is to provide enough tests to fit the second-order model correlating the key electroplating variables and the composition of Sn–Zn deposits close to the eutectic point. Based on the results and discussion in previous section, the experimental settings of run 15 in Table 3 are used as the central (original) point in the central composite design (CCD) study. Note that factor D is not considered in this CCD study because the deposits with composition very close to the metal ion ratio in the plating bath were preferred to prepare [19]. Thus, the $[\text{Sn}^{4+}]/[\text{Zn}^{2+}]$ ratio of the plating bath was kept constant ($[\text{Sn}^{4+}]/[\text{Zn}^{2+}] = 90/10$) in the CCD study.

A CCD study generally consists of a 2^m factorial design with $2m$ axial runs and n_C center runs. Hence, the total number of experimental runs in a CCD study is equal to $2^m + 2m + n_C$. For instance, factors A and C are considered in this CCD study. The total number of experimental runs in this CCD study is equal to $2^2 + 2 \times 2 + 3 = 11$. Since the distance from the experimental points to the central points is constant ($\sqrt{2}$ in this case), this design will have a constant variance of the response variable at all experimental points when the design is rotated about the origin [16].

Table 5

Design matrix and experimental data for the average Sn content in the Sn–Zn deposits for the central composite design with a quadratic form fit

Run	Factor		Sn content (wt%)
	A (pH)	C (T, °C)	
1	+1 (7.0)	+1 (78.0)	92.5
2	$+\sqrt{2}$ (7.4)	0 (70.0)	92.6
3	+1 (7.0)	−1 (62.0)	95.3
4	0 (6.0)	$-\sqrt{2}$ (58.8)	90.2
5	−1 (5.0)	−1 (62.0)	90.3
6	$-\sqrt{2}$ (4.6)	0 (70.0)	85.8
7	−1 (5.0)	+1 (78.0)	82.9
8	0 (6.0)	$+\sqrt{2}$ (81.2)	88.8
9	0 (6.0)	0 (70.0)	86.0
10	0 (6.0)	0 (70.0)	86.5
11	0 (6.0)	0 (70.0)	86.9

The design matrix with the corresponding results in the CCD study is shown in Table 5. The step size of pH and the plating temperature is 1 and 8 °C, respectively. The experiments on the original (central) point are repeated three times in order to evaluate the pure error between each experiment. The regression analysis and ANOVA for the data shown in Table 5 were carried out and the resultant second-order model representing the dependence of the Sn content on factors A (pH) and C (temperature of the plating solution) was generated as follow:

$$y = 86.5 + 3.0x_A - 1.5x_C + 1.6x_A^2 + 1.7x_C^2 + 1.2x_Ax_C \quad (12)$$

where y , x_A and x_C are indicative of the Sn content, pH, and temperature of the plating bath, respectively. This fitting has an R^2 value of 0.90, indicating that Eq. (12) suitably describes the dependence of the Sn content on factors A and C.

The contour plots for the dependence of the Sn content in the Sn–Zn deposits on factors A and C were constructed by using the regression model (i.e., Eq. (12)) and a typical contour diagram is shown in Fig. 2. Note that a minimum (ca. 84 at%) of the Sn content in the deposits is located around the conditions at pH 5.0 and 78 °C. In addition, the Sn content increases slowly when pH and temperature of the plating solutions are increased and decreased simultaneously. Note that a plateau with very weak dependence of the Sn content on the pH and temperature of the plating solutions is clearly found around the minimum. This indicates that the Sn content around the minimum is very stable, which is good for production (i.e., the robust conditions). Unfortunately, the minimal Sn content is not close to the eutectic point (i.e., Sn–9Zn) and thus, an additional confirmation test has to be performed.

In order to demonstrate the robust property of the electroplating settings for the co-deposition of the eutectic Sn–Zn alloys, the dependence of the Sn content for various Sn–Zn deposits plated at pH 5.0 and temperature = 78 °C on the ratio of $[\text{Sn}^{4+}]/[\text{Zn}^{2+}]$ in the plating solutions was investigated (see Table 6). From this table, the Sn content in the Sn–Zn deposits is gradually increased from 83.4 to 97.8 wt% when the $[\text{Sn}^{4+}]/[\text{Zn}^{2+}]$ ratio in the plating solutions is steadily increased from 90/10 to 97/3. Note that the composition of a Sn–Zn deposit plated from the solution with the $[\text{Sn}^{4+}]/[\text{Zn}^{2+}]$ ratio of 93/7 is

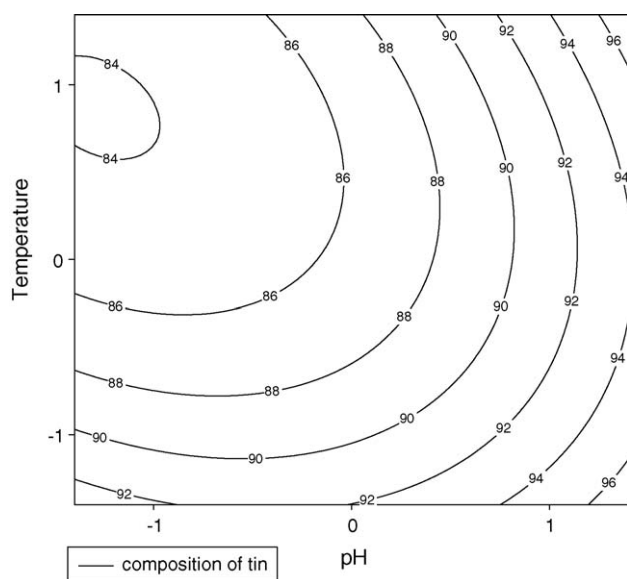


Fig. 2. Contour plots for the constant Sn contents in the Sn–Zn deposits against pH and temperature of the plating solutions.

approximately equal to the eutectic point (i.e., run 4 in Table 6). In addition, when the substrate was changed to be Ni/Cu or Cu, the composition of the Sn–Zn deposits prepared under the conditions of run 4 in Table 6 is still very close to the eutectic point (i.e., 90.8 and 90.9 wt% of Sn for the Ni/Cu and Cu substrates). The above results indicate that pH of 5.0 and temperature of 78 °C are the robust conditions for the co-deposition of Sn–Zn alloys with their composition close to the eutectic point, which is weakly dependent on the temperature and pH of the plating solutions.

3.3. Morphology and crystalline structure of Sn–Zn deposits

The morphologies of Sn–Zn deposits with the Sn content of ca. 83, 90, and 97 wt% are shown in Fig. 3. In general, these binary Sn–Zn deposits show polyhedral crystallites. In addition, the surface of these binary Sn–Zn deposits becomes smoother and compacter with increasing the Sn content although all deposits are micro-rough. Moreover, the Sn–Zn deposits with

Table 6

The dependence of the Sn content in the Sn–Zn deposits on the ratio of $[Sn^{4+}]/[Zn^{2+}]$ in the plating baths

Run	$[Sn^{4+}]/[Zn^{2+}]$	Sn content (wt%)
1	90/10	83.4
2	91/9	86.9
3	92/8	89.8
4	93/7	91.2
5	94/6	93.0
6	95/5	95.2
7	96/4	96.7
8	97/3	97.8

Remark: pH 5.0; temperature, 78 °C; total concentration of metal ions, 0.2 M; agitation rate, 10 rpm; current density, 80 mA/cm². All Sn–Zn deposits were electroplated at 80 mA/cm² under pH of 5.0 and 78 °C for 20 min.

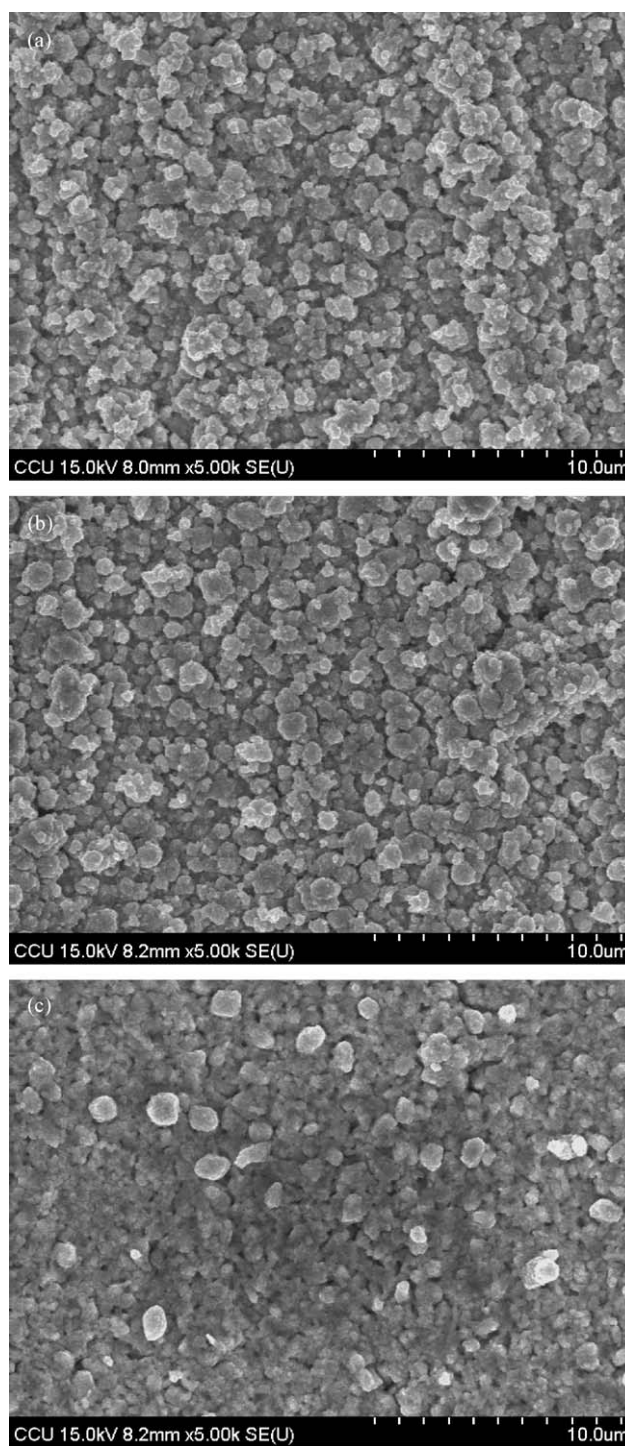


Fig. 3. The morphologies of Sn–Zn deposits with the Sn content of (a) 83, (b) 90, and (c) 97 wt%.

90 and 97 wt% Sn mainly consist of spherical grains. Since the morphology of these deposits shows the intimate mixing and uniting of Sn and Zn, the binary Sn–Zn deposits should belong to the heterogeneous alloys [14,24].

Fig. 4 shows the XRD patterns of Sn–Zn deposits with the Sn content of ca. 83, 90, and 97 wt%. On curve 1, there are several diffraction peaks corresponding to the crystalline faces of β -Sn, Zn, and Cu on this binary deposit, indicating that the

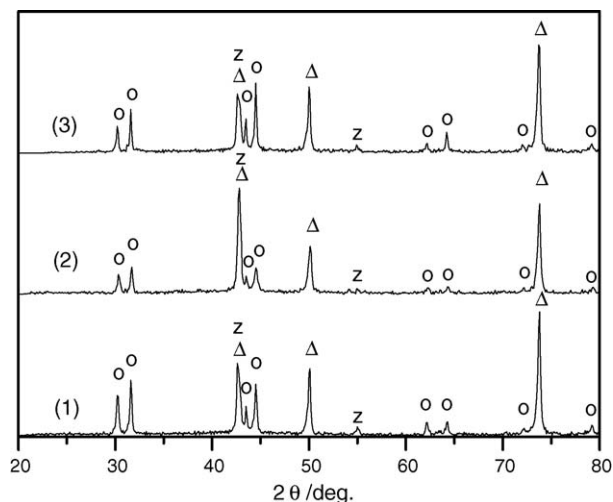


Fig. 4. The XRD patterns of Sn–Zn deposits with the Sn content of (1) 83, (2) 90, and (3) 97 wt%; where o, z, and Δ indicate the diffraction faces of Sn, Zn, and Cu, respectively.

Sn–Zn deposit with 83 wt% Sn is composed of polycrystalline Sn and Zn metals. In addition, the diffraction peaks corresponding to the crystalline faces of Zn are still visible for the Sn–Zn deposit with 3 wt% (see curve 3 in Fig. 4). This indicates that the concentration of Zn atoms dispersed in this deposit is still high enough to exhibit constructive diffraction although the intensity of the Zn diffraction peaks is very low for all deposits.

Based on all the above textural results, the Sn–Zn deposits prepared in this work should belong to heterogeneous alloys since Sn and Zn are mutually dissolved each other [14,24]. Moreover, the eutectic Sn–9Zn deposit can be easily electroplated under our reliable plating conditions although some studies reported the presence of eutectic-type Sn–Zn alloys with ca. 20 or 10 wt% Zn [25,26].

4. Conclusions

Using the sequential experiment strategies (i.e., the fractional factorial design and the central composite design coupled with response surface methodology), the robust deposition settings for the electroplating of Sn–Zn deposits with the composition close to the eutectic point (i.e., Sn–9Zn) were clearly demonstrated. The experimental settings, pH of 5.0, the total concentration of 0.2 M, the plating temperature of 78 °C, the $[\text{Sn}^{4+}]/[\text{Zn}^{2+}]$ ratio of 93/7, and the agitation rate of 10 rpm, for the plating of Sn–9Zn deposits were very robust to the Fe/Cu, Ni/Cu, and Cu substrates. Based on the robust plating settings proposed in this work, the composition of Sn–Zn alloys can be precisely con-

trolled by adjusting the composition of the plating baths. From the SEM and XRD results, the binary Sn–Zn deposits prepared in this work should belong to heterogeneous alloys.

Acknowledgment

The financial support of this work, by the National Science Council of the Republic of China, is gratefully acknowledged.

References

- [1] E.M. Davis, W.E. Harding, R.S. Schwartz, J.J. Corning, *IBM J. Res. Dev.* (1964) 102.
- [2] M. Carano, *Plat. Surf. Finish.* 91 (2004) 36.
- [3] C. VanHorn, R. Oberle, G. Shawhan, *Packaging, Production Conference—Proceedings of the Technical Program (West and East)*, vol. 1, 1997, p. 336.
- [4] P. Bratin, E. Shalyt, M. Pavlov, J. Berkman, *Proceedings of the IEEE/CPMT International Electronics Manufacturing Technology (IEMT) Symposium*, 2003, p. 395.
- [5] M. Carano, *Plat. Surf. Finish.* 90 (2003) 44.
- [6] P.A. Kohl, *J. Electrochem. Soc.* 129 (1982) 1196.
- [7] S. Arai, H. Akatsuka, N. Kaneko, *J. Electrochem. Soc.* 150 (2003) C730.
- [8] S. Joseph, G.J. Phatak, T. Seth, K. Gurunathan, D.P. Amalnerkar, T.R.N. Kutty, *IEEE Region 10 Annual International Conference Proceedings/TENCON*, vol. 4, 2003, p. 1367.
- [9] O. Khaselev, I.S. Zavarine, Vysotskaya, C. Fan, Y. Zhang, J. Abys, *Trans. Inst. Met. Finish.* 80 (2002) 200.
- [10] I. Yanada, D. Gudczauskas, *Proceedings of the AESF Annual Technical Conference*, 1999, p. 457.
- [11] E. Jung, R. Aschenbrenner, Ch. Kallmayer, P. Coskina, H. Reichl, *Proceedings of the International Symposium and Exhibition on Advanced Packaging Materials Processes Properties and Interfaces*, 2001, p. 119.
- [12] R. Kiumi, J. Yoshioka, F. Kuriyama, N. Saito, M. Shimoyama, *Proceedings—Electronic Components and Technology Conference*, 2002, p. 711.
- [13] J. Horkans, *J. Electrochem. Soc.* 128 (1981) 45.
- [14] A. Brenner, *Electrodeposition of Alloys*, vols. 1 and 2, Academic Press, New York/London, 1963.
- [15] J.A. Cornall, *How to Apply Response Surface Methodology*, vol. 8, ASQC, Wisconsin, 1990.
- [16] D.C. Montgomery, *Design and Analysis of Experiments*, fifth ed., J. Wiley & Sons, Singapore, 1997.
- [17] G.E.P. Box, W.G. Hunter, J.S. Hunter, *Statistics for Experiments*, J. Wiley & Sons, New York, 1978, p. 374.
- [18] C.-C. Hu, A. Bai, *Surf. Coat. Technol.* 137 (2001) 181.
- [19] P. Tsay, C.-C. Hu, *J. Electrochem. Soc.* 149 (2002) C492.
- [20] C.-C. Hu, T.-W. Tsou, *J. Power Sources* 115 (2003) 179.
- [21] J.W. Cuthbertson, R.M. Angles, *J. Electrochem. Soc.* 94 (1948) 73.
- [22] A.E. Davies, R.M. Angles, *Trans. Inst. Met. Finish.* 33 (1956) 277.
- [23] K. Aotani, *J. Electrochem. Soc. Jpn.* 21 (1953) 21.
- [24] K. Wang, H.W. Pickering, K.G. Weil, *Electrochim. Acta* 46 (2001) 3835.
- [25] E. Gaus, J. Torrent-Burgues, *J. Electroanal. Chem.* 549 (2003) 25.
- [26] K.-Y. Kim, Y. Yang, *Surf. Coat. Technol.* 64 (1994) 99.